



Predicting Hygroscopic Growth of Organosulfur Aerosol Particles Using COSMOtherm

Zijun Li¹, Angela Buchholz², and Noora Hyttinen³

¹International Laboratory for Air Quality and Health, School of Earth and Atmospheric Sciences, Queensland University of Technology, Brisbane QLD 4001, Australia

²Department of Technical Physics, University of Eastern Finland, Kuopio FI-70210, Finland

³Department of Chemistry, Nanoscience Center, University of Jyväskylä, Jyväskylä FI-40014, Finland

Correspondence: Zijun Li (zijun.li@qut.edu.au) and Noora Hyttinen (noora.x.hyttinen@jyu.fi)

Abstract. Organosulfur (OS) compounds are important sulfur species in atmospheric aerosol particles, due to the reduction of global inorganic sulfur emissions. Understanding the physicochemical properties, such as hygroscopicity, of OS compounds is important for predicting future aerosol-cloud-climate interactions. However, their hygroscopicity is not yet well understood due to the scarcity of authentic standards. In this work, we investigated a group of OS compounds and their mixtures with ammonium sulfate, for which the hygroscopic growth factors (HGF) have been experimentally studied. Here, the HGFs were calculated from water activities computed using the conductor-like screening model for real solvents (COSMO-RS). A good agreement was found between the model-estimated and experimental HGFs for the studied OS compounds. This quantum-chemistry-based approach for HGF estimation will open up the possibility of investigating the hygroscopicity of other OS compounds present in the atmosphere.

10 1 Introduction

Atmospheric aerosol particles affect the global climate directly by scattering solar radiation or indirectly by seeding clouds. As important aerosol constituents, organosulfur (OS) compounds contribute up to 30% of total organic aerosol particles in mass (Surratt et al., 2008; Tolocka and Turpin, 2012). Typically, these OS compounds contain a sulfonate or sulfate ester group. Methanesulfonic acid, the most abundant OS compound in marine environments, can be produced via both gas and aqueous-phase oxidation of reduced-sulfur compounds (Barnes et al., 2006; Hoffmann et al., 2016; Berndt et al., 2023). Another OS compound of high abundance (Moch et al., 2020), namely hydroxymethanesulfonate, is formed from sulfite and formaldehyde in the aqueous phase (Boyce and Hoffmann, 1984; Song et al., 2019). Moreover, other OS compounds can be formed via multi-phase oxidation of biogenic but also anthropogenic organic compounds in the presence of sulfuric acid. To date, OS compounds have been identified in various environments across forest (Iinuma et al., 2007; Kristensen and Glasius, 2011), coastal (Huang et al., 2015; Zhou et al., 2023), polar (Hansen et al., 2014; Ye et al., 2019; Campbell et al., 2022), and urban sites (Jiang et al., 2022; Glasius et al., 2022). Therefore, the abundance and ubiquity of OS compounds in the atmosphere highlight their importance for global climate.



Understanding the interactions of OS compounds with water vapor as a function of relative humidity (RH) is important in assessing their climate effect. When in equilibrium with surrounding RH, the degree of water uptake (i.e., hygroscopicity) largely affects aerosol phase states, optical properties, chemical reactivity, and cloud formation potential. A range of laboratory studies have investigated the hygroscopicity for both commercially available and synthesized OS compounds under sub-saturated (RH<100%) conditions (Hansen et al., 2015; Estillore et al., 2016; Peng et al., 2021, 2022; Ohno et al., 2022; Bain et al., 2023). Inorganic salts typically show distinct deliquescence and efflorescence RH (DRH and ERH) points, while the studied OS compounds consistently show continuous growth with increasing RH. Furthermore, the presence of OS compounds can lower the DRH and ERH of inorganic salt particles (Estillore et al., 2016; Peng et al., 2021, 2022), and potentially extends the RH range where particulate water is present and thus influences the physicochemical properties of atmospheric aerosol particles.

Both Aerosol Inorganic-Organic Mixtures Functional Groups Activity Coefficients (AIOMFAC) (Zuend et al., 2008, 2011; Zuend and Seinfeld, 2012) and conductor-like screening model for real solvents (COSMO-RS) (Klamt, 1995; Klamt et al., 1998; Eckert and Klamt, 2002) can estimate the activity coefficients of compounds present in atmospheric aerosol particles as a function of RH. Recently, the solubilities and activities of isoprene- and monoterpene-derived organosulfates were computed using COSMO-RS (Hytinen et al., 2020). To our knowledge, there is, however, no comparison between the experimental and thermodynamic model-estimated hygroscopicity of OS compounds, which become increasingly important due to declining SO₂ emissions (Riva et al., 2019). This hinders the understanding of their atmospheric impacts and fates.

Here, we perform quantum chemistry calculations with COSMO-RS to explore a set of atmospherically relevant OS compounds (Table S1 in the Supplement), including

- Sodium OS: methyl sulfate (NaMS), hydroxymethanesulfonate (NaHMS), ethyl sulfate (NaES), and 2-hydroxyethylsulfonate (NaHES)
- Potassium OS: glycolic acid sulfate (KGAS), hydroxyacetone sulfate (KHAS), 2-butenediol sulfate (KBS), and 4-hydroxy-2,3-epoxybutane sulfate (KHEBS)
- Ammonium OS: 2-hydroxyethyl-sulfonate (NH₄HES), (2R,3S)-1,3,4-trihydroxy-2-methylbutan-2-yl sulfate (NH₄TMS (a)), and (2R,3R)-2,3,4-trihydroxy-2-methylbutan-2-yl sulfate (NH₄TMS (b)).

The experimental hygroscopicities of these OS are reported in the literature (Estillore et al., 2016; Peng et al., 2021, 2022; Ohno et al., 2022). For each studied OS, we estimate the corresponding water activities (α_w) at a range of solute concentrations to predict the hygroscopic growth curves. Additionally, we predict particle hygroscopicity for the OS mixed with ammonium sulfate (AS; (NH₄)₂SO₄), which is the most abundant inorganic salt in atmospheric aerosol particles.



2 Computational methods

2.1 Activity coefficients

The COSMO-RS model (Klamt, 1995; Klamt et al., 1998; Eckert and Klamt, 2002), implemented in the BIOVIA COSMO*therm* program (BIOVIA COSMO*therm*, 2021) (abbreviated COSMO*therm*), was used to calculate activity coefficients of water. All activity coefficients were calculated using the most recent BP_TZVPD_FINE_21 parametrization (abbreviated FINE), with the exception of solutions containing AS, which were calculated using the newly developed electrolyte parametrization BP_TZVP_ELYTE_21 (abbreviated ELYTE; see Section S1 in the Supplement for more details). The activity coefficient γ_i of a compound j is computed using the pseudo-chemical potential μ^* (Ben-Naim, 1987) at composition \mathbf{x} and at the reference state \mathbf{x}° :

$$\ln \gamma_j(\mathbf{x}) = \frac{\mu_j^*(\mathbf{x}) - \mu_j^{*,\circ}(\mathbf{x}^\circ, T, P)}{RT} \quad (1)$$

where T is the temperature (295 K), R the gas constant (in $\text{kJ K}^{-1}\text{mol}^{-1}$) and $P = 10^5$ Pa is the reference pressure. The pseudo-chemical potential μ_j^* is an auxiliary quantity defined using the chemical potential at the reference state μ° :

$$\mu_j^*(\mathbf{x}) = \mu_j^\circ(\mathbf{x}^\circ, T, P) + RT \ln \gamma_j(\mathbf{x}) \quad (2)$$

Pure water with mole fraction (x_w) of 1 is used as the reference state composition \mathbf{x}° . With the calculated γ_j , each aqueous-phase composition is paired with a RH assuming that at equilibrium, $\alpha_w = \text{RH}/100\%$, where $\alpha_w = x_w \gamma_w$.

2.2 Input files for COSMO*therm* calculations

Input files for COSMO*therm* calculations (cosmo-files) were obtained through a series of density functional theory calculations with increasing levels of theory. The process has been discussed in more detail in a previous publication (Hytinen et al., 2020). In short, all conformers were found using the systematic conformer search algorithm in the Spartan20 program (Wavefunction Inc., 2020). The geometries of all conformers were optimized and duplicate conformers were removed using the BIOVIA COSMO*conf* program (BIOVIA COSMO*conf*, 2021; TURBOMOLE, 2020). The final cosmo-files were computed at the BP/def2-TZVPD-FINE//BP/def-TZVP level of theory (BP/def-TZVP for BP_TZVP_ELYTE_21 calculations).

Many of the studied cations have multiple conformers. At most 10 lowest chemical potential conformers were selected as inputs for the COSMO*therm* calculations. However, only conformers with chemical potentials within 8 kJ mol^{-1} of the lowest chemical potential were used, in order to avoid including conformers with low COSMO energies but high chemical potentials (Hytinen, 2023). More specifically, COSMO*therm* gives high weights to conformers containing intramolecular H-bonds (Hytinen and Prisle, 2020), because intramolecular H-bonds are favored in the COSMO energies (Kurtén et al., 2018).

2.3 Predicting HGF of OS particles

The hygroscopicity of an organic compound is typically quantified using the hygroscopic growth factor (HGF), which is the ratio of the diameter at a RH condition i ($D_{p,i}$) to the diameter at dry conditions ($\text{RH} \leq 10\%$; $D_{p,0}$):



$$\text{HGF} = \frac{D_{p,i}}{D_{p,0}} \quad (3)$$

Assuming particle sphericity, HGF can be further expressed with:

$$\text{HGF} = \left(\frac{V_{p,i}}{V_{p,0}} \right)^{\frac{1}{3}} \quad (4)$$

85 where $V_{p,i}$ and $V_{p,0}$ are the particle volumes at RH condition i and dry conditions, respectively. Assuming volume additivity, HGF can be represented using the volume of water and the solute (V_{OS} and V_{H_2O}).

$$\text{HGF} = \left(\frac{V_{OS} + V_{H_2O,i}}{V_{OS} + V_{H_2O,0}} \right)^{\frac{1}{3}} \quad (5)$$

The volume of each component j (V_j) can be written using the mass at RH = i ($m_{j,i}$) and density ρ_j :

$$V_j = \frac{m_{j,i}}{\rho_j} \quad (6)$$

90 Combing Eqs. 5 and 6 leads to:

$$\text{HGF} = \left(\frac{\frac{m_{OS}}{\rho_{OS}} + \frac{m_{H_2O,i}}{\rho_{H_2O}}}{\frac{m_{OS}}{\rho_{OS}} + \frac{m_{H_2O,0}}{\rho_{H_2O}}} \right)^{\frac{1}{3}} = \left(\frac{1 + \frac{m_{H_2O,i} \cdot \rho_{OS}}{m_{OS} \cdot \rho_{H_2O}}}{1 + \frac{m_{H_2O,0} \cdot \rho_{OS}}{m_{OS} \cdot \rho_{H_2O}}} \right)^{\frac{1}{3}} \quad (7)$$

where the mass ratio between m_{H_2O} and m_{OS} can be predicted using the COSMO $therm$ -estimated mass fraction of water at equilibrium.

2.4 Predicting HGF of OS-AS mixture particles

95 COSMO $therm$ calculations assume that all salts are dissolved in water regardless of the water content. However, AS may exist in the solid state in aqueous mixtures under low RH conditions. When the RH increases above the DRH, AS reaches its solubility limit and undergoes a solid-to-liquid phase transition. At the DRH, the molar ion activity product (IAP) of the inorganic salt (e.g., AS) will be the same, regardless of other components in the mixture. It is therefore possible to determine the DRH of different salt mixtures, if the IAP of the inorganic salt for one saturated solution (IAP $_{sat}$) can be calculated.

100 For a specific ion, the molal activity coefficient $\gamma_{j,b}$ can be computed using the mole fraction-based activity coefficient $\gamma_{j,x}$ estimated by COSMO $therm$ (Robinson and Stokes, 2002):

$$\gamma_{j,b} = \frac{\gamma_{j,x}}{1 + 0.001 \cdot MW \cdot \sum_j \nu_j b_j} \quad (8)$$

where MW is the molar mass of the solvent water, ν_j is the number of moles of ions formed by the ionization of one mole of salt j (3 for AS and 2 for OS) and b_j is the molality (i.e., moles of solute per kg of water) of salt j . The IAP of AS in a solution
105 can be calculated using the molal ionic activity coefficients and molalities of NH_4^+ and SO_4^{2-} (Robinson and Stokes, 2002):



$$IAP = [\gamma_{\text{NH}_4^+, b} \cdot b_{\text{NH}_4^+}]^2 [\gamma_{\text{SO}_4^{2-}, b} \cdot b_{\text{SO}_4^{2-}}]^{-1} \quad (9)$$

The IAP_{sat} is calculated using the aqueous solubility limit of AS (i.e., 5.790 mol AS per kg of water at 295 K). When the estimated $IAP > IAP_{sat}$, AS is assumed to exist only in its solid form. In this case, the OS is the sole component contributing to the particle water uptake. Under such a condition, we apply the Zdanovskii–Stokes–Robinson (ZSR) approach Stokes and
110 Robinson (1966) to estimate the particle water uptake, assuming no interactions between AS and the aqueous phase. The corresponding HGF of the OS-AS mixture is derived by multiplying the COSMO $_{therm}$ -estimated HGF for the pure OS with the OS volume fraction in the OS-AS mixture.

3 Results and discussion

3.1 Water activity of OS

115 α_w of the studied OS were estimated in solutions with water mass fractions (m_w) ranging from 0 to 0.96 (Fig. 1). Since different OS have different molecular weights, using m_w enables a direct comparison of the water uptake for the studied salts. All OS are assumed to be fully dissolved in the water as ions. Due to the scarcity of experimental data on α_w for the studied OS, it is not possible to determine the relative errors of the model estimates.

In the sodium OS group, the studied OS with the same carbon number exhibit higher m_w with more oxygenated functional
120 groups at a fixed α_w below 0.7 (i.e., RH below 70%). In the potassium OS group, the selected OS display higher m_w with increasing molecular weights at a fixed α_w . The three chosen ammonium OS show similar degrees of water uptake, independent of the anion. When comparing the three cation groups (i.e., Na^+ , K^+ , and NH_4^+), we observed that at a fixed α_w , the group of potassium OS (Fig. 1b) shows the lowest degree of water uptake as indicated by the lowest m_w . Note that most of the anions are different between the three cation groups. The difference in α_w between the three cation groups can arise from the differences
125 in cations and/or anions.

To rule out the effect of cations, we additionally computed the α_w for all cation-anion pairs (Fig. S2 in the Supplement). Re-
130 gardless of the anion, at any α_w , potassium OS show the lowest m_w , as compared to the corresponding sodium and ammonium OS. Note that at $\alpha_w \leq 0.7$, most sodium OS have lower equilibrium water content compared to the corresponding ammonium OS. However, at $\alpha_w > 0.7$, both sodium and ammonium OS show similar equilibrium water content for each of the studied anions.

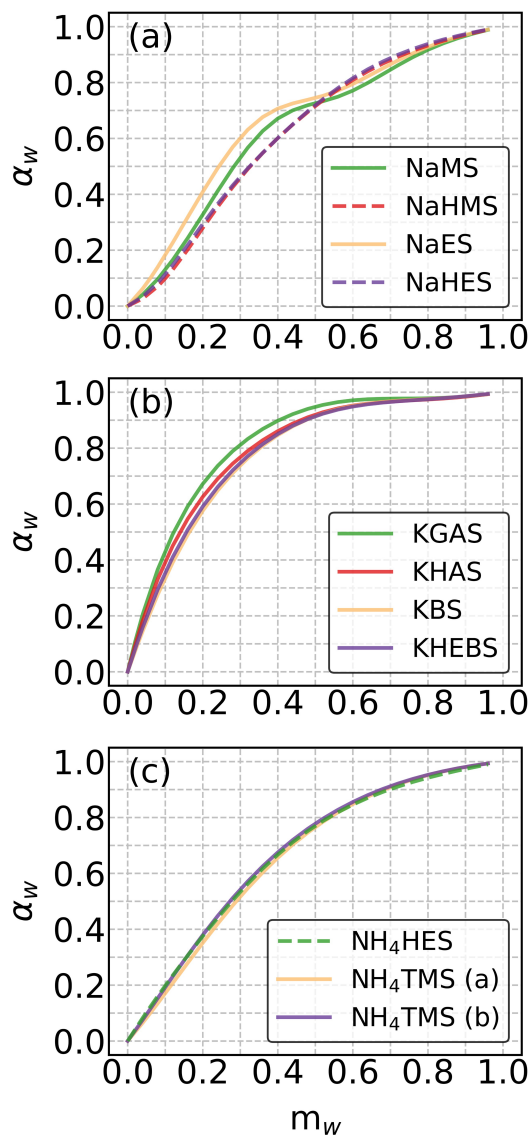


Figure 1. COSMO $therm$ -derived water activities (α_w) in aqueous solutions of the studied (a) sodium, (b) potassium, (c) and ammonium OS as a function of water mass fraction (m_w) at 295 K. The solid and dashed lines represent salts of organosulfates and organosulfonates, respectively.

3.2 Hygroscopicity of OS particles

We calculated the HGF for each studied OS, on the basis of the COSMO $therm$ -estimated m_w and density (ρ , Table S1 in the Supplement). The corresponding COSMO $therm$ -estimated HGFs with the experimental data are shown for three selected OS (i.e., NaMS, KGAS, and NH₄HES) particles in Fig. 2. Both the measured and computed HGFs are very similar to each other.

135 Fig. S3 in the Supplement summarizes the experimental and computed HGF data of all the studied OS particles as a function



of RH. Note that the COSMO $therm$ -predicted HGFs mostly agree with the measurement data. This agreement highlights the validation of using m_w and ρ from COSMO $therm$ to predict the hygroscopic growth of OS particles.

In addition, we compared the HGF data using all three available parametrizations of the COSMO- $therm$ program (FINE, TZVP, and ELYTE), as shown in Fig. S4 in the Supplement. For the four studied sodium OS particles, ELYTE gave similarly good or even better HGF estimates, compared to FINE. For the potassium OS particles, the FINE HGF estimates show the best agreement with the literature data, compared to the TZVP and ELYTE estimates. When considering the three studied ammonium OS particles, the three parametrizations provided similar RH-dependency of HGFs but gave only reasonably good HGF estimates for NH₄HES particles. Among the three COSMO $therm$ parametrizations, FINE overall provided the best agreement across all the studied OS particles and was thus chosen for the detailed analysis.

We acknowledge that the effect of surface tension was not taken into account in the HGF calculation for each studied OS. However, considering the dry OS particle size of 100 nm or larger from the experimental studies, the surface tension effect can be assumed to be negligible in the sub-saturated regime (Bezantakos et al., 2016). For smaller particles and surface-active compounds, the surface tension may significantly affect the equilibrium water content.

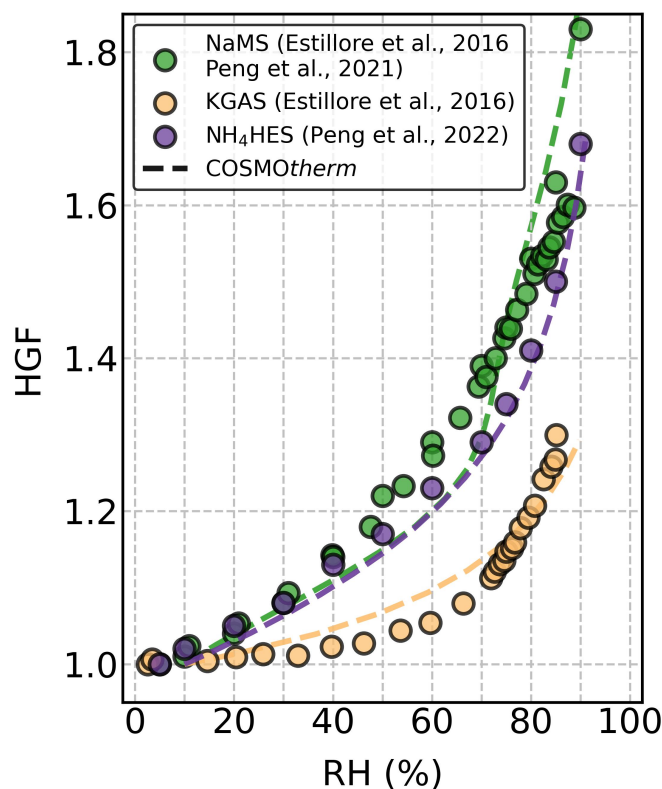


Figure 2. Hygroscopic growth factors (HGFs) for sodium methyl sulfate (NaMS; green), potassium glycolic acid sulfate (KGAS; yellow), and ammonium 2-hydroxyethyl-sulfonate (NH₄HES; purple) as a function of RH at 295 K. The HGF data from the literature (Estillore et al., 2016; Peng et al., 2021, 2022) and the COSMO $therm$ -derived calculations are shown in solid circles and dashed lines, respectively.



3.3 Hygroscopicity of OS-AS mixture particles

150 We also examined the RH dependency of HGF for the studied OS-AS mixture particles at mass ratios (OS:AS) of 1:1, 1:3, and 1:5. Fig. 3 shows the ZSR-predicted HGF as a function of RH for the three methyl sulfate (MS) salts mixed with AS. Whenever available, the corresponding experimental HGF data are presented as well. For other OS-AS mixture particles, the HGF data are presented in Fig. S5 in the Supplement.

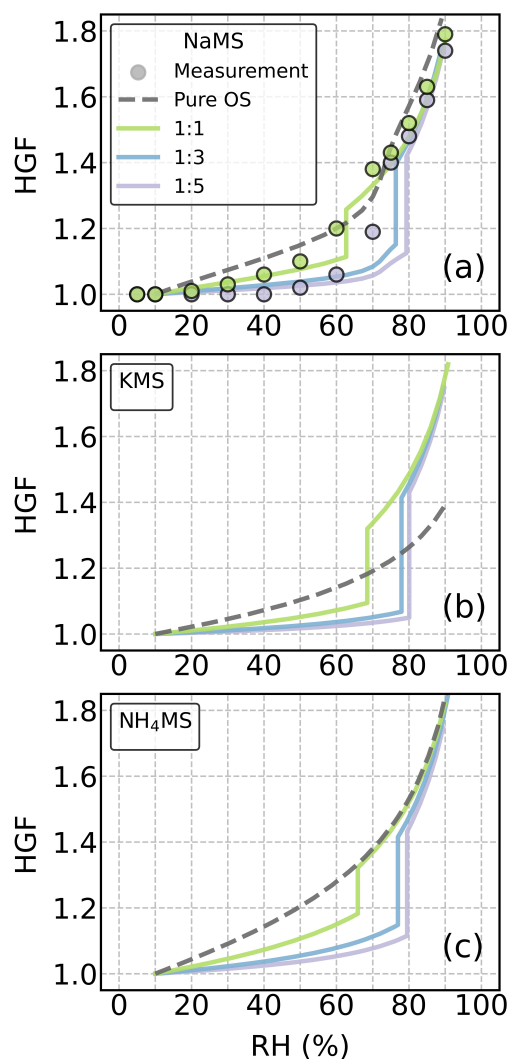


Figure 3. Hygroscopic growth factors (HGFs) of the mixture particles of ammonium sulfate (AS) and (a) sodium, (b) potassium and (c) ammonium methyl sulfate as a function of RH at 295 K. The filled circles indicate measurement data from the literature (Estillore et al., 2016; Peng et al., 2021). The HGF data derived from the COSMO_{therm}-based calculations are in dashed lines for pure organosulfur (OS) compounds and in solid lines for the OS-AS mixed particles. Colors indicate different OS:AS mass ratios.



The estimated HGF show that unlike the pure MS particles (grey dashed lines in Fig. 3), almost all the MS-AS mixture particles (solid lines) with the three chosen mass ratios exhibited gradual water uptake behaviours and then sharp deliquescence transitions at 60 % RH or above. With an increasing mass fraction of AS in the solute, the DRH of the MS-AS mixture particles shifts to higher RH but is still lower than the DRH of the pure AS (i.e., 80% RH). The presence of AS noticeably lowered water uptake compared to the pure OS cases when RH was below the DRH. Similar results were observed in other OS-AS mixture particles (Fig. S5). However, when RH was above the DRH, the addition of AS only increases water uptake of KMS and other potassium OS particles.

Our HGF estimates are able to reproduce the measured HGF curves of the NaMS-AS mixture particles with 1:1 mass ratio (Fig. 3a). For the NaMS-AS mixture particles with 1:3 mass ratio, the HGF estimate well predicts the measurement data at $RH < 60\%$ or $RH > 80\%$ but there is disagreement around the DRH. Similar HGF underestimation at 60%–80% RH was also observed in NaHMS, NaHES, NaES and NH_4 HES mixture particles with AS with 1:3 and 1:5 mass ratios. For these 1:3 and 1:5 OS-AS mixture particles, the discrepancy between the measured and estimated HGFs is likely due to the underestimated interaction between MS and AS near the deliquescence phase transition and the resultant overestimated IAP of AS. It is also possible that solid AS partially dissolves into the aqueous phase before the onset of deliquescence, thus leading to higher HGF at 60%–80% RH than expected. Such partial dissolution behavior of AS is not accounted for in our approach when the IAP of AS is below IAP_{sat} .

4 Conclusions

This novel approach does not require any reference OS data for optimization prior to HGF estimations. Instead, it is solely based on the quantum chemistry calculations and existing parametrizations of the commercially available COSMO $therm$ program. Our benchmarking shows good agreement between COSMO $therm$ -derived and experimental HGFs in most cases of the studied OS.

Globally, SO_2 emissions are projected to decrease due to the phasing out of fossil fuels. This is expected to decrease the total and inorganic sulfur, thereby increasing the contribution of OS to total sulfur in atmospheric aerosol particles (Riva et al., 2019; Brüggemann et al., 2020). With progress in analytical instruments and methods, hundreds of OS compounds have been recently identified from field measurements (Hettiyadura et al., 2017, 2019; Wang et al., 2021; Huang et al., 2023; Wang et al., 2023; Yang et al., 2023). However, investigation of the physicochemical properties of OS is still lacking due to the scarcity of authentic standards. Our COSMO $therm$ -based approach allows characterizing the hygroscopicity of OS particles even when authentic standards are unavailable. This will help us understand the aerosol-cloud-climate interactions in the post-fossil-fuel future where OS compounds are highly important.

<https://doi.org/10.5194/egusphere-2024-1182>

Preprint. Discussion started: 7 May 2024

© Author(s) 2024. CC BY 4.0 License.



Data availability. The data set is available upon request from the corresponding author.

Author contributions. ZL and NH conceived the study. ZL performed the data collection and hygroscopicity calculation. NH performed the
185 COSMOtherm calculations. ZL, AB, and NH analyzed and interpreted data. ZL wrote the paper with contributions from all coauthors

Competing interests. The author has declared that there are no competing interests.

Acknowledgements. ZL thanks the QUT Early Career Research Scheme for funding support. NH thanks the Research Council of Finland, Grant No. 338171, for the financial contribution and CSC—IT Center for Science, Finland, for the computational resources. We thank Dr Henry Oswin for the helpful discussion.



190 References

- Bain, A., Chan, M. N., and Bzdek, B. R.: Physical properties of short chain aqueous organosulfate aerosol, *Environ. Sci.: Atmos.*, 3, 1365–1373, 2023.
- Barnes, I., Hjorth, J., and Mihalopoulos, N.: Dimethyl sulfide and dimethyl sulfoxide and their oxidation in the atmosphere, *Chem. Rev.*, 106, 940–975, 2006.
- 195 Ben-Naim, A.: *Solvation Thermodynamics*, Plenum Press, New York and London, 1987.
- Berndt, T., Hoffmann, E. H., Tilgner, A., Stratmann, F., and Herrmann, H.: Direct sulfuric acid formation from the gas-phase oxidation of reduced-sulfur compounds, *Nat. Commun.*, 14, 4849, 2023.
- Bezantakos, S., Huang, L., Barmounis, K., Martin, S. T., and Biskos, G.: Relative humidity non-uniformities in hygroscopic tandem differential mobility analyzer measurements, *J. Aerosol Sci.*, 101, 1–9, 2016.
- 200 BIOVIA COSMOconf: Dassault Systèmes, available at: <http://www.3ds.com>, last access: 29 January 2021, 2021.
- BIOVIA COSMOtherm: Release 2021, Dassault Systèmes, available at: <http://www.3ds.com>, last access: 1 April 2021, 2021.
- Boyce, S. D. and Hoffmann, M. R.: Kinetics and mechanism of the formation of hydroxymethanesulfonic acid at low pH, *J. Phys. Chem.*, 88, 4740–4746, 1984.
- Brüggemann, M., Xu, R., Tilgner, A., Kwong, K. C., Mutzel, A., Poon, H. Y., Otto, T., Schaefer, T., Poulain, L., Chan, M. N., and Herrmann, H.: Organosulfates in ambient aerosol: state of knowledge and future research directions on formation, abundance, fate, and importance, *Environ. Sci. Technol.*, 54, 3767–3782, 2020.
- 205 Campbell, J. R., Battaglia Jr, M., Dingilian, K., Cesler-Maloney, M., St Clair, J. M., Hanisco, T. F., Robinson, E., DeCarlo, P., Simpson, W., Nenes, A., Weber, R. J., and Mao, J.: Source and Chemistry of Hydroxymethanesulfonate (HMS) in Fairbanks, Alaska, *Environ. Sci. Technol.*, 56, 7657–7667, 2022.
- 210 Eckert, F. and Klamt, A.: Fast solvent screening via quantum chemistry: COSMO-RS approach, *AIChE J.*, 48, 369–385, <https://doi.org/10.1002/aic.690480220>, 2002.
- Estillore, A. D., Hettiyadura, A. P. S., Qin, Z., Leckrone, E., Wombacher, B., Humphry, T., Stone, E. A., and Grassian, V. H.: Water Uptake and Hygroscopic Growth of Organosulfate Aerosol, *Environ. Sci. Technol.*, 50, 4259–4268, <https://doi.org/10.1021/acs.est.5b05014>, 2016.
- Glasius, M., Thomsen, D., Wang, K., Iversen, L. S., Duan, J., and Huang, R.-J.: Chemical characteristics and sources of organosulfates, organosulfonates, and carboxylic acids in aerosols in urban Xi'an, Northwest China, *Sci. Total Environ.*, 810, 151 187, 2022.
- 215 Hansen, A., Kristensen, K., Nguyen, Q., Zare, A., Cozzi, F., Nøjgaard, J., Skov, H., Brandt, J., Christensen, J., Ström, J., Tunved, P., Krejci, R., and Glasius, M.: Organosulfates and organic acids in Arctic aerosols: speciation, annual variation and concentration levels, *Atmos. Chem. Phys.*, 14, 7807–7823, 2014.
- Hansen, A. M. K., Hong, J., Raatikainen, T., Kristensen, K., Ylisirniö, A., Virtanen, A., Petäjä, T., Glasius, M., and Prisle, N. L.: Hygroscopic properties and cloud condensation nuclei activation of limonene-derived organosulfates and their mixtures with ammonium sulfate, *Atmos. Chem. Phys.*, 15, 14 071–14 089, <https://doi.org/10.5194/acp-15-14071-2015>, 2015.
- 220 Hettiyadura, A. P., Jayarathne, T., Baumann, K., Goldstein, A. H., de Gouw, J. A., Koss, A., Keutsch, F. N., Skog, K., and Stone, E. A.: Qualitative and quantitative analysis of atmospheric organosulfates in Centreville, Alabama, *Atmos. Chem. Phys.*, 17, 1343–1359, 2017.
- Hettiyadura, A. P. S., Al-Naiema, I. M., Hughes, D. D., Fang, T., and Stone, E. A.: Organosulfates in Atlanta, Georgia: anthropogenic influences on biogenic secondary organic aerosol formation, *Atmos. Chem. Phys.*, 19, 3191–3206, 2019.
- 225



- Hoffmann, E. H., Tilgner, A., Schrödner, R., Brüner, P., Wolke, R., and Herrmann, H.: An advanced modeling study on the impacts and atmospheric implications of multiphase dimethyl sulfide chemistry, *Proc. Natl. Acad. Sci. U. S. A.*, 113, 11 776–11 781, 2016.
- Huang, D. D., Li, Y. J., Lee, B. P., and Chan, C. K.: Analysis of organic sulfur compounds in atmospheric aerosols at the HKUST supersite in Hong Kong using HR-ToF-AMS, *Environ. Sci. Technol.*, 49, 3672–3679, 2015.
- 230 Huang, L., Wang, Y., Zhao, Y., Hu, H., Yang, Y., Wang, Y., Yu, J.-Z., Chen, T., Cheng, Z., Li, C., Li, Z., and Xiao, H.: Biogenic and Anthropogenic Contributions to Atmospheric Organosulfates in a Typical Megacity in Eastern China, *Geophys. Res. Atmos.*, 128, e2023JD038 848, 2023.
- Hytinen, N.: Predicting liquid-liquid phase separation in ternary organic-organic-water mixtures, *Phys. Chem. Chem. Phys.*, 25, 11 121–11 129, 2023.
- 235 Hytinen, N. and Prisle, N. L.: Improving solubility and activity estimates of multifunctional atmospheric organics by selecting conformers in COSMOtherm, *J. Phys. Chem. A*, 124, 4801–4812, <https://doi.org/10.1021/acs.jpca.0c04285>, 2020.
- Hytinen, N., Elm, J., Malila, J., Calderón, S. M., and Prisle, N. L.: Thermodynamic properties of isoprene- and monoterpene-derived organosulfates estimated with COSMOtherm, *Atmos. Chem. Phys.*, 20, 5679–5696, <https://doi.org/10.5194/acp-20-5679-2020>, 2020.
- Iinuma, Y., Müller, C., Berndt, T., Böge, O., Claeys, M., and Herrmann, H.: Evidence for the existence of organosulfates from β -pinene
- 240 ozonolysis in ambient secondary organic aerosol, *Environ. Sci. Technol.*, 41, 6678–6683, 2007.
- Jiang, H., Li, J., Tang, J., Cui, M., Zhao, S., Mo, Y., Tian, C., Zhang, X., Jiang, B., Liao, Y., Chen, Y., and Zhang, G.: Molecular characteristics, sources, and formation pathways of organosulfur compounds in ambient aerosol in Guangzhou, South China, *Atmos. Chem. Phys.*, 22, 6919–6935, 2022.
- Klamt, A.: Conductor-like screening model for real solvents: a new approach to the quantitative calculation of solvation phenomena, *J. Phys. Chem.*, 99, 2224–2235, <https://doi.org/10.1021/j100007a062>, 1995.
- 245 Klamt, A., Jonas, V., Bürger, T., and Lohrenz, J. C. W.: Refinement and parametrization of COSMO-RS, *J. Phys. Chem. A*, 102, 5074–5085, <https://doi.org/10.1021/jp980017s>, 1998.
- Kristensen, K. and Glasius, M.: Organosulfates and oxidation products from biogenic hydrocarbons in fine aerosols from a forest in North West Europe during spring, *Atmos. Environ.*, 45, 4546–4556, 2011.
- 250 Kurtén, T., Hytinen, N., D’Ambro, E. L., Thornton, J., and Prisle, N. L.: Estimating the saturation vapor pressures of isoprene oxidation products $C_5H_{12}O_6$ and $C_5H_{10}O_6$ using COSMO-RS, *Atmos. Chem. Phys.*, 18, 17 589–17 600, <https://doi.org/10.5194/acp-18-17589-2018>, 2018.
- Moch, J. M., Dovrou, E., Mickley, L. J., Keutsch, F. N., Liu, Z., Wang, Y., Dombek, T. L., Kuwata, M., Budisulistiorini, S. H., Yang, L., Decesari, S., Paglione, M., Alexander, B., Shao, J., Munger, J. W., and Jacob, D. J.: Global importance of hydroxymethanesulfonate in
- 255 ambient particulate matter: Implications for air quality, *Geophys. Res. Atmos.*, 125, e2020JD032 706, 2020.
- Ohno, P. E., Wang, J., Mahrt, F., Varelak, J. G., Aruffo, E., Ye, J., Qin, Y., Kiland, K. J., Bertram, A. K., Thomson, R. J., and Martin, S. T.: Gas-Particle Uptake and Hygroscopic Growth by Organosulfate Particles, *ACS Earth Space Chem.*, 6, 2481–2490, <https://doi.org/10.1021/acsearthspacechem.2c00195>, 2022.
- Peng, C., Razafindrambinina, P. N., Malek, K. A., Chen, L., Wang, W., Huang, R.-J., Zhang, Y., Ding, X., Ge, M., Wang, X., Asa-Awuku, A. A., and Tang, M.: Interactions of organosulfates with water vapor under sub- and supersaturated conditions, *Atmos. Chem. Phys.*, 21, 7135–7148, <https://doi.org/10.5194/acp-21-7135-2021>, 2021.



- Peng, C., Malek, K. A., Rastogi, D., Zhang, Y., Wang, W., Ding, X., Asa-Awuku, A. A., Wang, X., and Tang, M.: Hygroscopicity and cloud condensation nucleation activities of hydroxyalkylsulfonates, *Sci. Total Environ.*, 830, 154767, <https://doi.org/https://doi.org/10.1016/j.scitotenv.2022.154767>, 2022.
- 265 Riva, M., Chen, Y., Zhang, Y., Lei, Z., Olson, N. E., Boyer, H. C., Narayan, S., Yee, L. D., Green, H. S., Cui, T., Zhang, Z., Baumann, K., Fort, M., Edgerton, E., Budisulistiorini, S. H., Rose, C. A., Ribeiro, I. O., e Oliveira, R. L., dos Santos, E. O., Machado, C. M. D., Szopa, S., Zhao, Y., Alves, E. G., de Sá, S. S., Hu, W., Knipping, E. M., Shaw, S. L., Duvoisin Junior, S., de Souza, R. A. F., Palm, B. B., Jimenez, J.-L., Glasius, M., Goldstein, A. H., Pye, H. O. T., Gold, A., Turpin, B. J., Vizuete, W., Martin, S. T., Thornton, J. A., Dutcher, C. S., Ault, A. P., and Surratt, J. D.: Increasing isoprene epoxydiol-to-inorganic sulfate aerosol ratio results in extensive conversion of inorganic sulfate to organosulfur forms: implications for aerosol physicochemical properties, *Environ. Sci. Technol.*, 53, 8682–8694, 2019.
- 270 Robinson, R. A. and Stokes, R. H.: *Electrolyte solutions*, Courier Corporation, 2002.
- Song, S., Gao, M., Xu, W., Sun, Y., Worsnop, D. R., Jayne, J. T., Zhang, Y., Zhu, L., Li, M., Zhou, Z., Cheng, C., Lv, Y., Wang, Y., Peng, W., Xu, X., Lin, N., Wang, Y., Wang, S., Munger, J. W., Jacob, D. J., and McElroy, M. B.: Possible heterogeneous chemistry of hydroxymethanesulfonate (HMS) in northern China winter haze, *Atmos. Chem. Phys.*, 19, 1357–1371, 2019.
- 275 Stokes, R. H. and Robinson, R. A.: Interactions in aqueous nonelectrolyte solutions. I. Solute-solvent equilibria, *J. Phys. Chem.*, 70, 2126–2131, 1966.
- Surratt, J. D., Gómez-González, Y., Chan, A. W. H., Vermeylen, R., Shahgholi, M., Kleindienst, T. E., Edney, E. O., Offenberg, J. H., Lewandowski, M., Jaoui, M., Maenhaut, W., Claeys, M., Flagan, R. C., and Seinfeld, J. H.: Organosulfate formation in biogenic secondary organic aerosol, *J. Phys. Chem. A*, 112, 8345–8378, 2008.
- 280 Tolocka, M. P. and Turpin, B.: Contribution of organosulfur compounds to organic aerosol mass, *Environ. Sci. Technol.*, 46, 7978–7983, 2012.
- TURBOMOLE: V7.5.1, a development of University of Karlsruhe and Forschungszentrum Karlsruhe GmbH, 1989–2007, TURBOMOLE GmbH, since 2007, 2020.
- Wang, Y., Zhao, Y., Wang, Y., Yu, J.-Z., Shao, J., Liu, P., Zhu, W., Cheng, Z., Li, Z., Yan, N., and Xiao, H.: Organosulfates in atmospheric aerosols in Shanghai, China: seasonal and interannual variability, origin, and formation mechanisms, *Atmos. Chem. Phys.*, 21, 2959–2980, 2021.
- Wang, Y., Liang, S., Le Breton, M., Wang, Q. Q., Liu, Q., Ho, C. H., Kuang, B. Y., Wu, C., Hallquist, M., Tong, R., and Yu, J. Z.: Field observations of C₂ and C₃ organosulfates and insights into their formation mechanisms at a suburban site in Hong Kong, *Sci. Total Environ.*, 904, 166851, 2023.
- 290 Wavefunction Inc.: *Spartan’20*, Irvine, CA, 2020.
- Yang, T., Xu, Y., Ye, Q., Ma, Y.-J., Wang, Y.-C., Yu, J.-Z., Duan, Y.-S., Li, C.-X., Xiao, H.-W., Li, Z.-Y., Zhao, Y., and Xiao, H.-Y.: Spatial and diurnal variations of aerosol organosulfates in summertime Shanghai, China: potential influence of photochemical processes and anthropogenic sulfate pollution, *Atmos. Chem. Phys.*, 23, 13433–13450, 2023.
- Ye, Y., Xie, Z., Zhu, M., and Wang, X.: Molecular Characterization of Organosulfates in Arctic Ocean and Antarctic atmospheric aerosols, *Atmos. Chem. Phys. Discuss. [preprint]*, pp. 1–24, 2019.
- 295 Zhou, S., Guo, F., Chao, C.-Y., Yoon, S., Alvarez, S. L., Shrestha, S., Flynn III, J. H., Usenko, S., Sheesley, R. J., and Griffin, R. J.: Marine submicron aerosols from the Gulf of Mexico: Polluted and acidic with rapid production of sulfate and organosulfates, *Environ. Sci. Technol.*, 57, 5149–5159, 2023.



- 300 Zuend, A. and Seinfeld, J. H.: Modeling the gas-particle partitioning of secondary organic aerosol: the importance of liquid-liquid phase separation, *Atmos. Chem. Phys.*, 12, 3857–3882, 2012.
- Zuend, A., Marcolli, C., Luo, B. P., and Peter, T.: A thermodynamic model of mixed organic-inorganic aerosols to predict activity coefficients, *Atmos. Chem. Phys.*, 8, 4559–4593, <https://doi.org/10.5194/acp-8-4559-2008>, 2008.
- 305 Zuend, A., Marcolli, C., Booth, A. M., Lienhard, D. M., Soonsin, V., Krieger, U. K., Topping, D. O., McFiggans, G., Peter, T., and Seinfeld, J. H.: New and extended parameterization of the thermodynamic model AIOMFAC: calculation of activity coefficients for organic-inorganic mixtures containing carboxyl, hydroxyl, carbonyl, ether, ester, alkenyl, alkyl, and aromatic functional groups, *Atmos. Chem. Phys.*, 11, 9155–9206, <https://doi.org/10.5194/acp-11-9155-2011>, 2011.